Ultrafast Optical Control of Semiconductor Spin Qubits toward Surface Code Quantum Computing

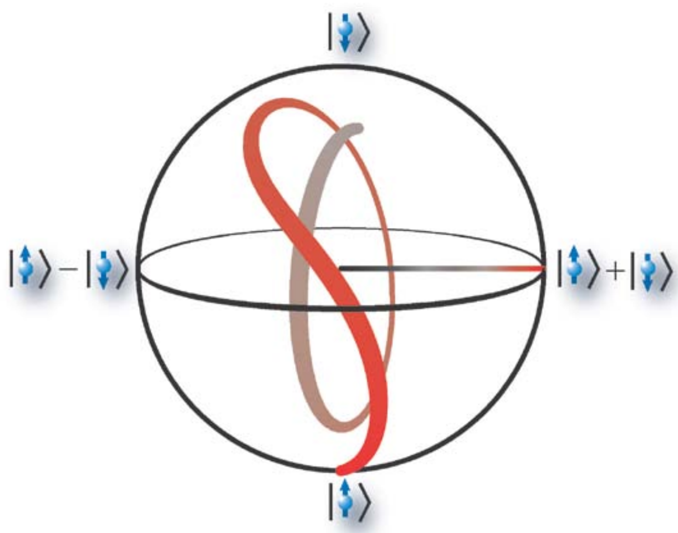

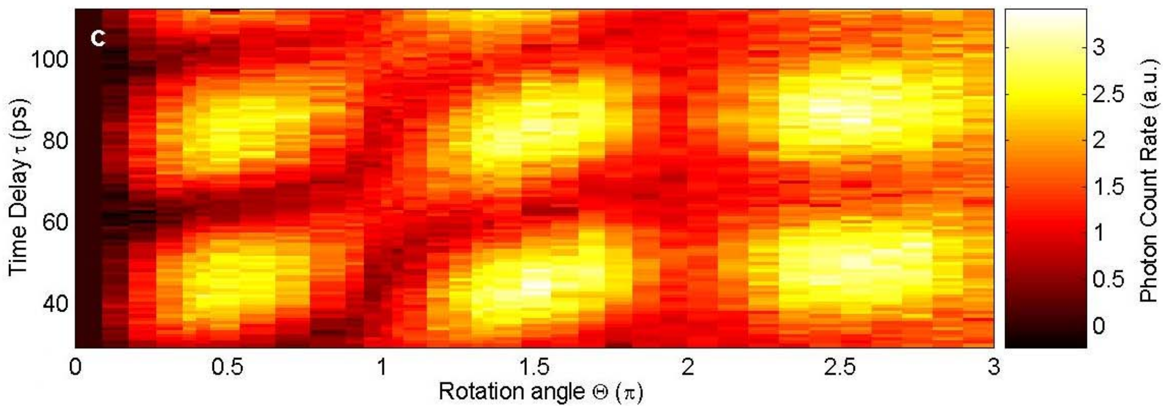

Yoshihisa Yamamoto
Stanford University & National Institute of Informatics

FIRST最先端研究開発支援プログラム　量子情報処理プロジェクト
第１回夏期研修会（沖縄、2010年8月18日～8月28日）

Outline

- Physical qubits – Quantum dot spins in planar microcavity –
- Goal – Fault tolerant quantum information processing –
- Qubit initialization and measurement
- Single qubit gate
- Two qubit gate
- Decoherence time
- Indistinguishable single photons and entanglement distribution
- Topological surface code architecture

Physical Qubits

— Cavity QED Systems with Single-Electron-Doped Quantum Dots —

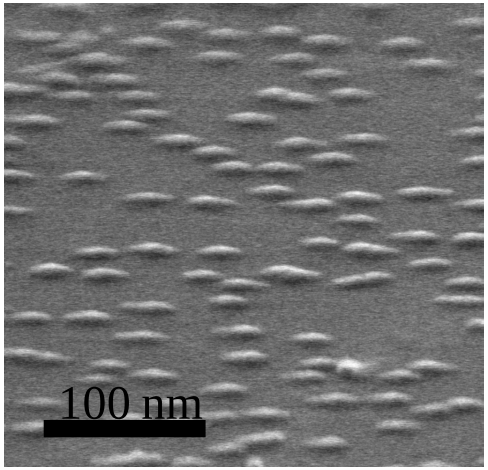

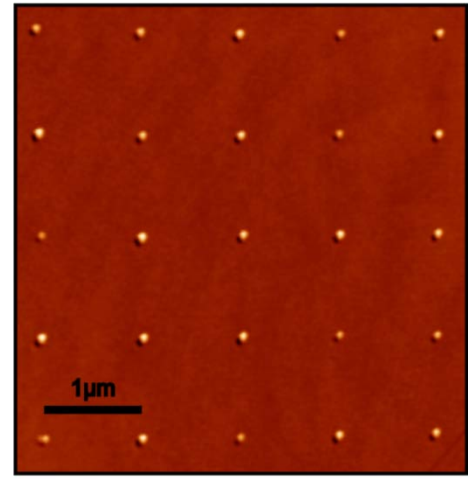

"Random" → **"Scalable"**

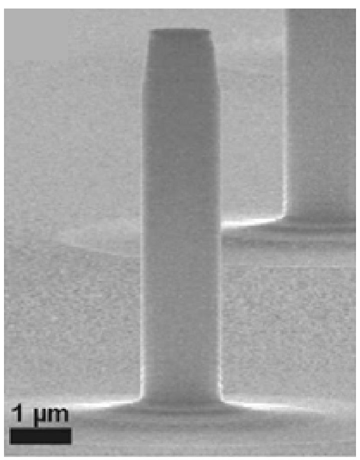

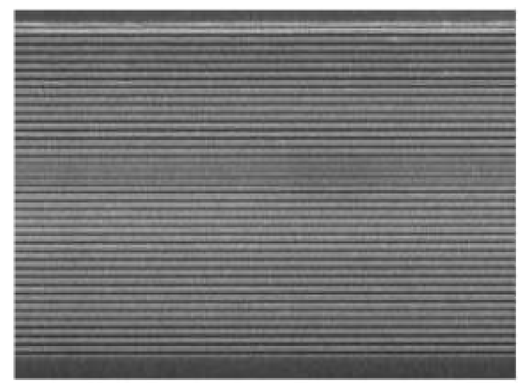

A post-microcavity with top and bottom DBRs and self-assembled InGaAs QDs

D. Press, S. Gotzinger, S. Reitzenstein, C. Hofmann, A. Loffler, M. Kamp, A. Forchel, and Y. Yamamoto, *PRL* **98**, 117402 (2007).

A simple planar microcavity with 2D lattice of site-controlled QDs

C. Schneider, M. Strauss, T. Sunner, A. Huggenberger, D. Wiener, S. Reitzenstein, M. Kamp, S. Hofling and A. Forchel *APL* **92**, 183101 (2008)

Single QD Cavity QED System with Enhanced Spontaneous Emission

D. Press et al. Phys. Rev. Lett. 98, 117402 (2007)

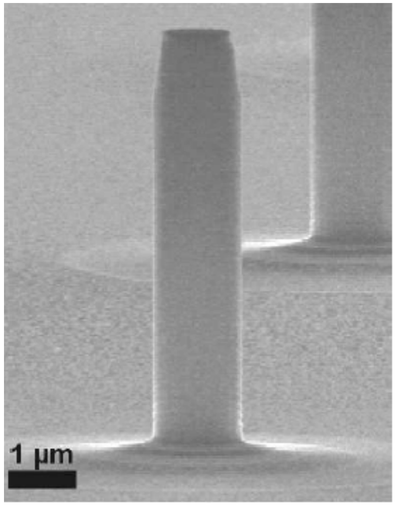

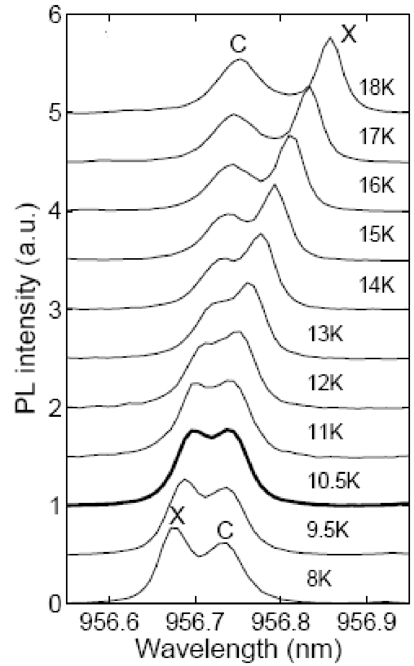

InAs QD exciton lifetime in free space 620ps

↓

Reduced lifetime in resonant cavity 11.3ps

↓

Purcell (cooperativity) factor $F_p = \frac{\gamma}{\gamma_x} - 1 = 61$

Quantum efficiency$= \frac{F_p}{F_p + 1} \times \frac{\gamma_c}{\gamma_c + \gamma_x} = 97\%$

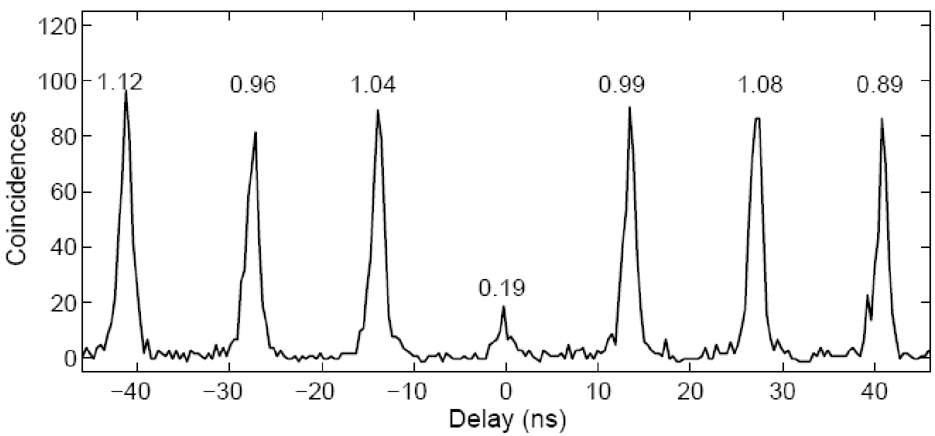

$g^{(2)}(0) = 0.19$ under resonant pumping

↓

Direct proof of a single QD cavity QED system

(Also see K. Hennessy et al., Nature 445, 896 (2007))

Magnetic Spectrum of Charged Exciton (Trion) in InAs Quantum Dot
― Artificial Three-Level Atom in Lambda Configuration ―

Magnetic field in Voigt geometry

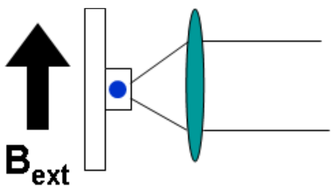

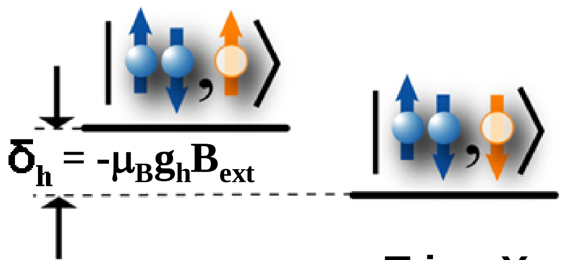

Trion X^-

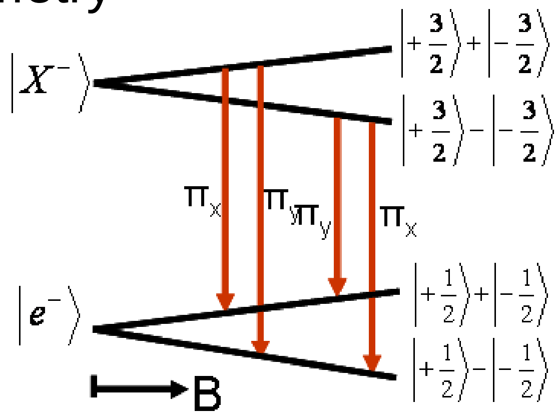

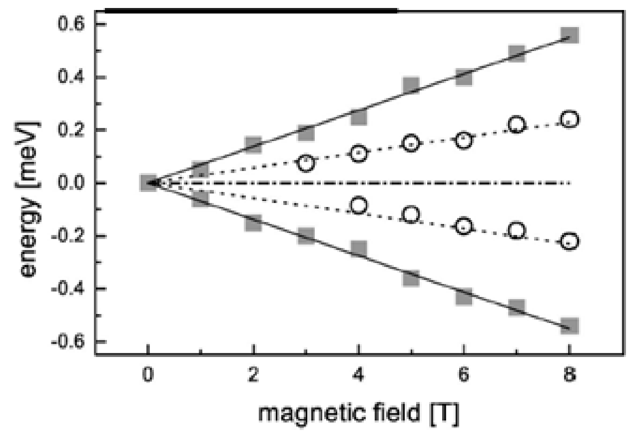

M. Bayer et al., Phys. Rev. B 65, 195305 (2002)

Electron spins in singlet
Spin is governed by heavy hole

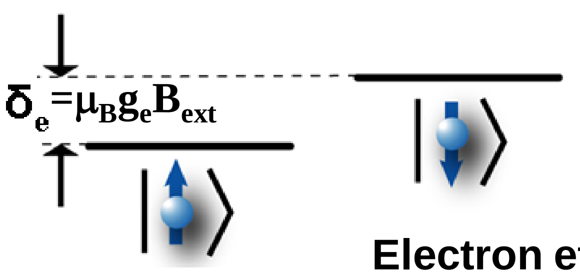

Electron e^-

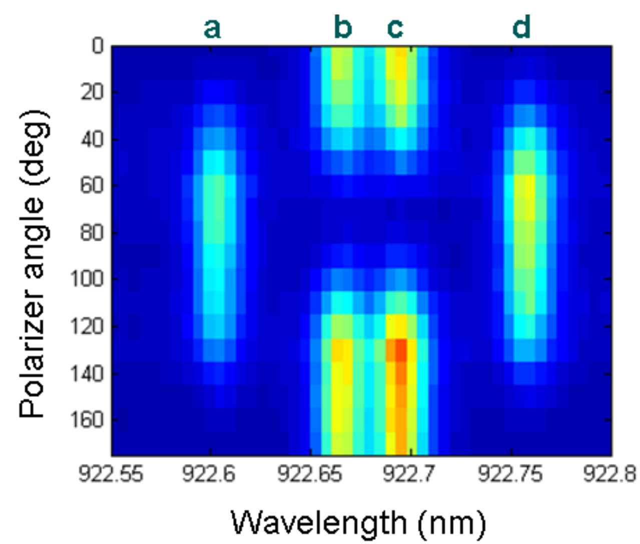

D. Press et al., Nature 456, 218 (2008)

Outline

- Physical qubits – Quantum dot spin lattice in planar microcavity –
- Goal – Fault tolerant quantum information processing –
- Qubit initialization and projective measurement
- Single qubit gate
- Two qubit gate
- Decoherence time
- Indistinguishable single photons and entanglement distribution
- Topological surface code architecture

Motivation － Why Optically Controlled QDs as Physical Qubits? －

Fault-tolerant quantum information processing systems

- Long distance quantum repeaters based on nested purification protocol
  Concept: H.J. Briegel, W. Dür, J.I. Cirac and P. Zoller, *PRL* **81**, 5932 (1998)
  Fault-tolerant Implementation with QD spins: T.D. Ladd, P. van Loock, K. Nemoto, W.J. Munro and Y. Yamamoto, *NJP* **8**, 184 (2006)

- One-way quantum computers based on topological surface codes
  Concept: R. Raussendorf and J. Harrington, *PRL* **98**, 190504 (2007)
  Fault-tolerant Implementation with QD spins: R. Van Meter, T.D. Ladd, A.G. Fowler and Y. Yamamoto, quant-ph/0906271 (2009)

Unique features of QDs as “artificial atoms”

i) Large oscillator strength: $f_{exciton} \geq 10\text{-}100 \times f_{atom}$
→ Ultrafast optical control with small optical power, large Purcell (cooperativity) factor

ii) Permanent placement of 2D spin lattice in monolithic planar microcavity
→ Scalable system (Unique mode spot size and cavity mediated one/two-qubit gate)

iii) Excitonic transition wavelength tailored to λ=1.3/1.5 μm
→ Natural interface to long-distance optical communication networks

Outline

- Physical qubits – Quantum dot spin lattice in planar microcavity –
- Motivation – Fault tolerant quantum information processing –
- Qubit initialization and measurement
- Single qubit gate
- Two qubit gate
- Decoherence time
- Indistinguishable single photons and entanglement distribution
- Topological surface code architecture

Initialization and Measurement of Electron Spins

Ensemble of spins: **K.M. Fu et al., Nature Physics 4, 780 (2008)**

Single spin: **D. Press et al., Nature 456, 218 (2008)**

Optical pumping + Rotation pulse of Θ = π

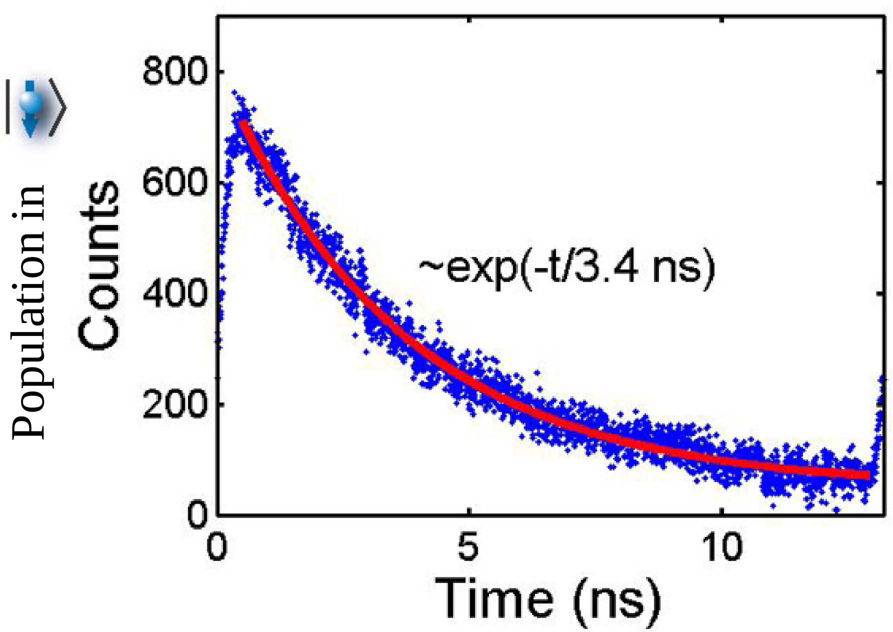

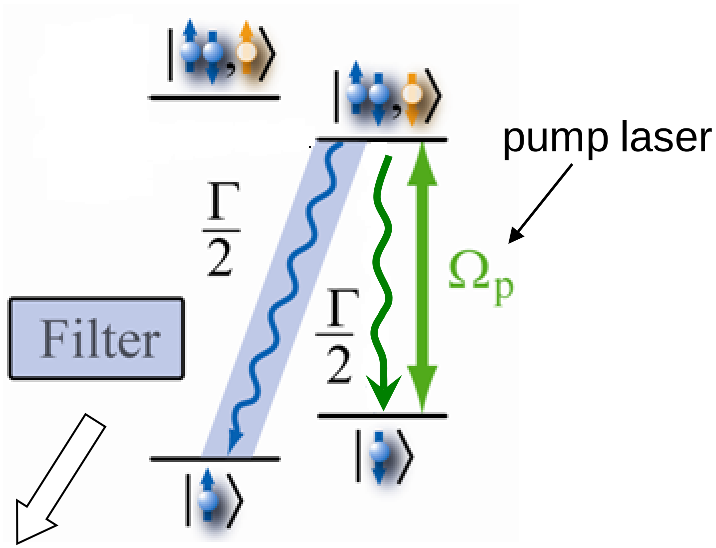

Single Photon Detection

T = 1.5 K, B_{ext} = 7 T

Initialization fidelity:
$F_0 = 92 \pm 7\%$

Time for initialization:
10^{-3}sec (thermalization scheme) → 10^{-9}sec (optical pumping)

Outline

- Physical qubits – Quantum dot spin lattice in planar microcavity –
- Motivation – Fault tolerant quantum information processing –
- Qubit initialization and projective measurement
- Single qubit gate
- Two qubit gate
- Decoherence time
- Indistinguishable single photons and entanglement distribution
- Topological surface code architecture

Spin Rotation with Single Optical Pulse
S. Clark et al., Phys. Rev. Lett. 99, 040501 (2007)

- A single broadband optical pulse can implement an arbitrary one-bit gate with fidelity of 0.999.

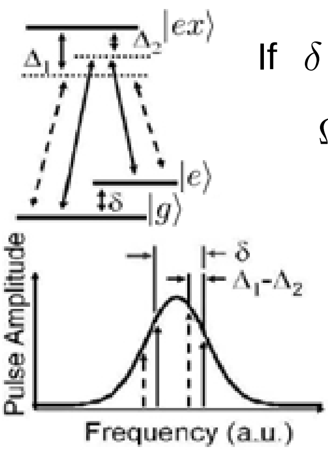

If $\delta \ll \Omega_0, \Omega_1 \ll \Delta,$ an effective Rabi frequency

$$\Omega_{\text{eff}} = \frac{\Omega_0 \Omega_1^*}{2\Delta} \simeq \frac{|\Omega(t)|^2}{2\Delta}$$

$$\Omega(t) = \frac{\mu E(t)}{\hbar}$$

rotation angle $\int \Omega_{\text{eff}}\, dt$ is proportional to pulse energy

Numerical simulation based on the three-level master equation

$$\tau \ll T_1, T_2$$

100fs π/2 - pulse

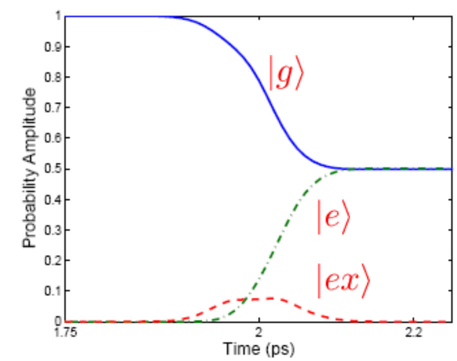

- A system clock is provided by the pulse arrival time from the mode-locked laser.

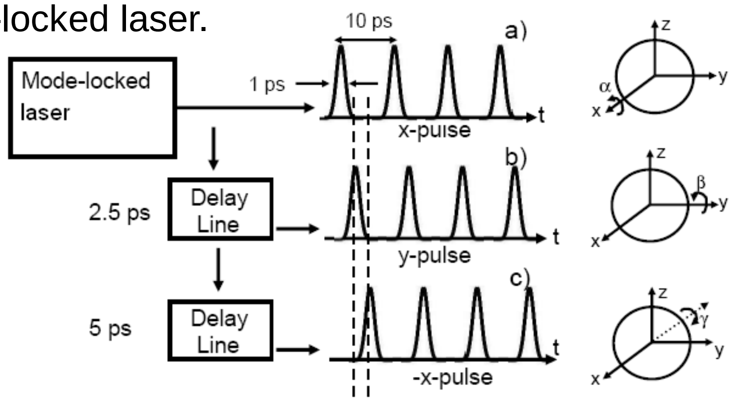

100fs π - pulse

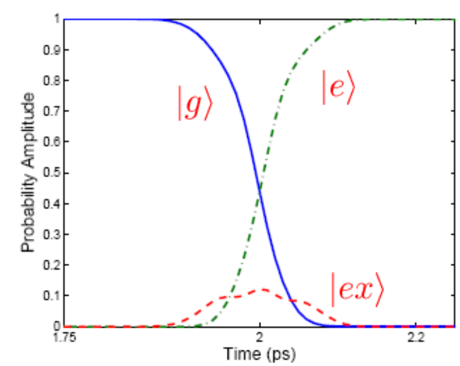

Arbitrary single qubit gates SU(2) can be implemented in one-half of Larmor oscillation period.

Experiment with an ensemble of donor spins : K.M. Fu et al., Nature Physics 4, 780 (2008)

Single Spin Experiment: Coherent Rabi Oscillation

D. Press et al., Nature 456, 218 (2008)

Circularly-polarized 4 ps Rotation Pulse

δ_e = 26 GHz
BW = 110 GHz
Δ = 270 GHz

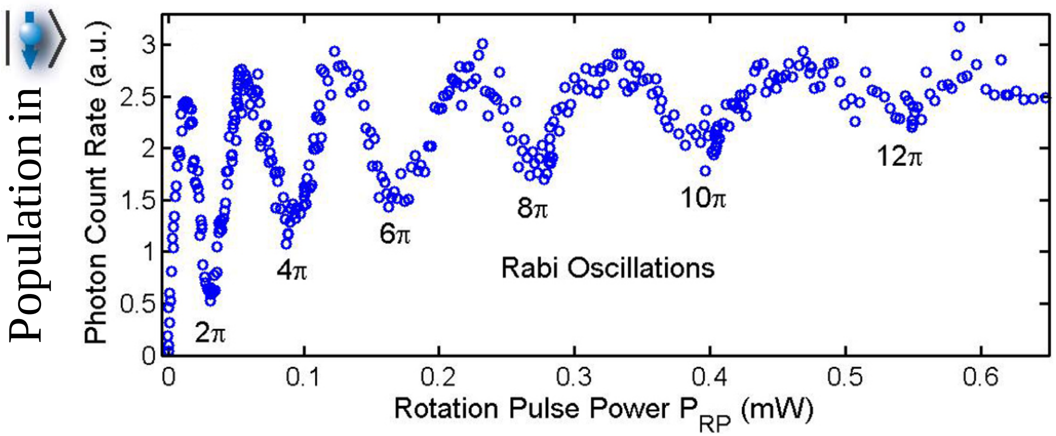

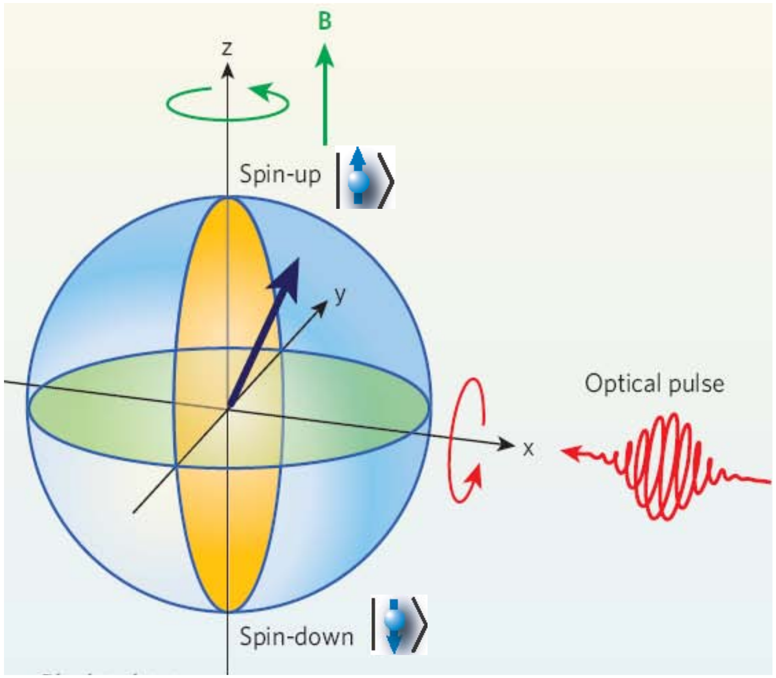

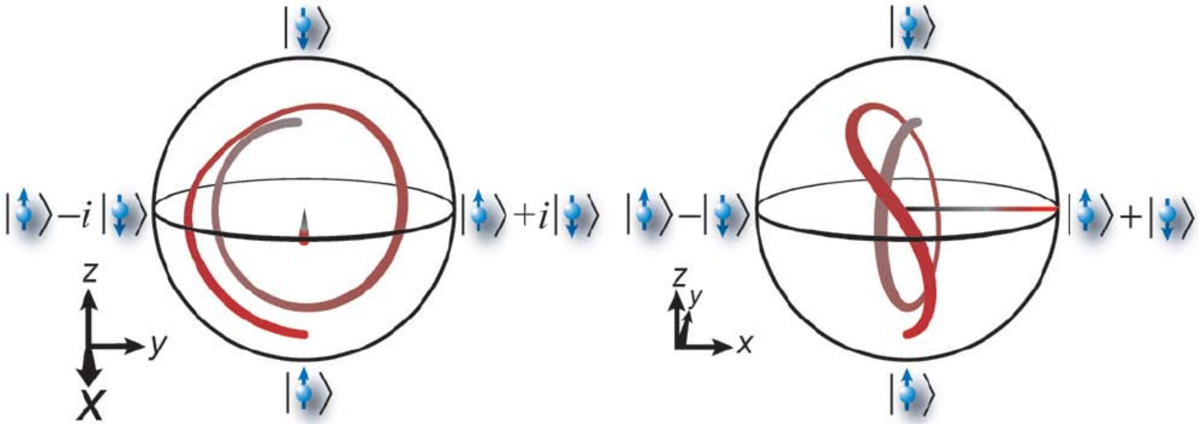

(cf. J. Berezovsky *et al.*, Science 320, 349 (2008))

Two-Pulse Experiment: Ramsey Interference

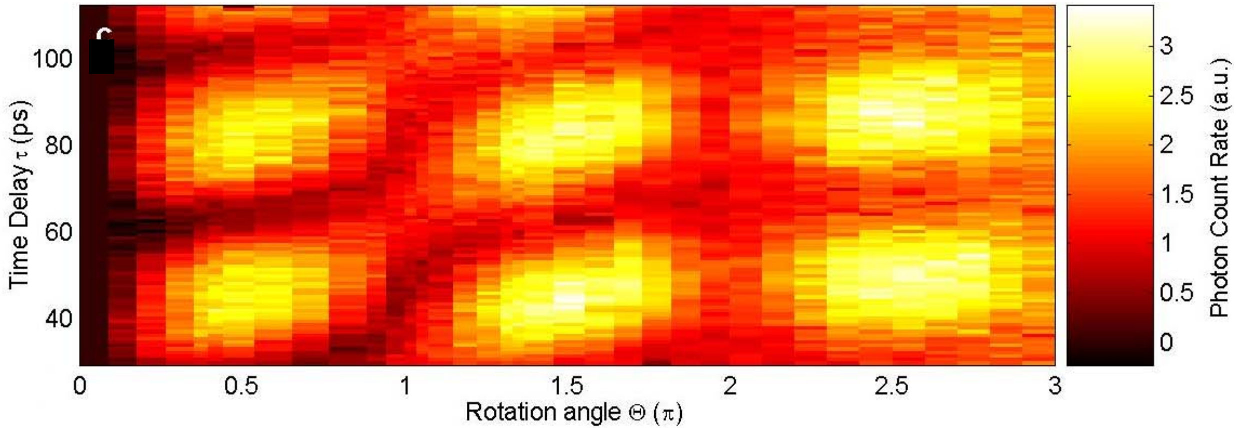

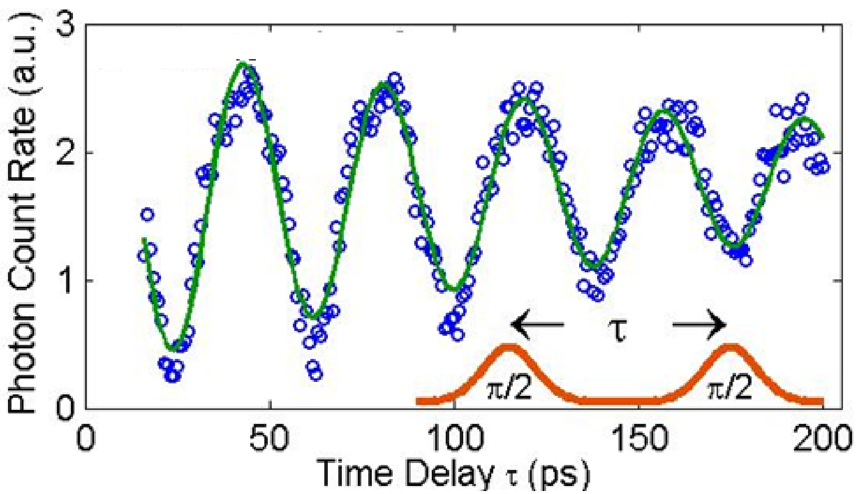

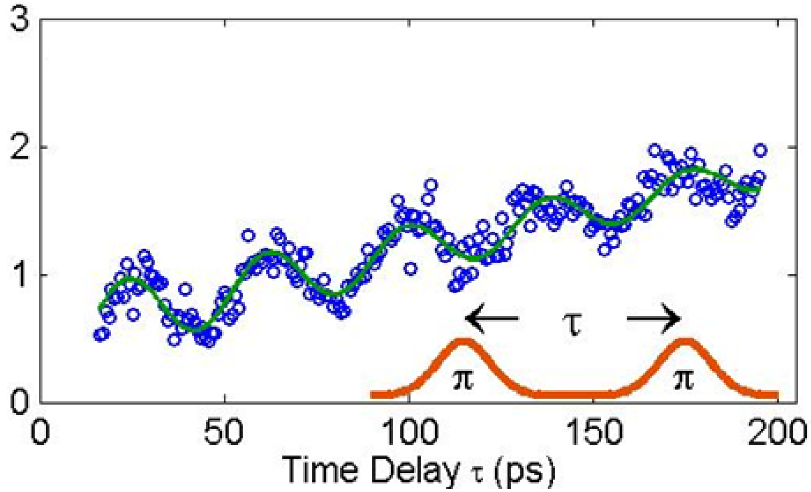

$\pi/2$-pulse fidelity: $F_{\pi/2}$ ~ 94%

π-pulse fidelity: F_{π} ~ 91%

Total time for SU(2) single qubit gates (≲ one-half of Larmor period)

D. Press *et al.*, Nature **456**, 218 (2008)

Improved Gate Fidelity for a Single Spin in a Microcavity
D. Press et al., Nature Photonics 4, 367 (2010)

Coherent Rabi oscillation experiment

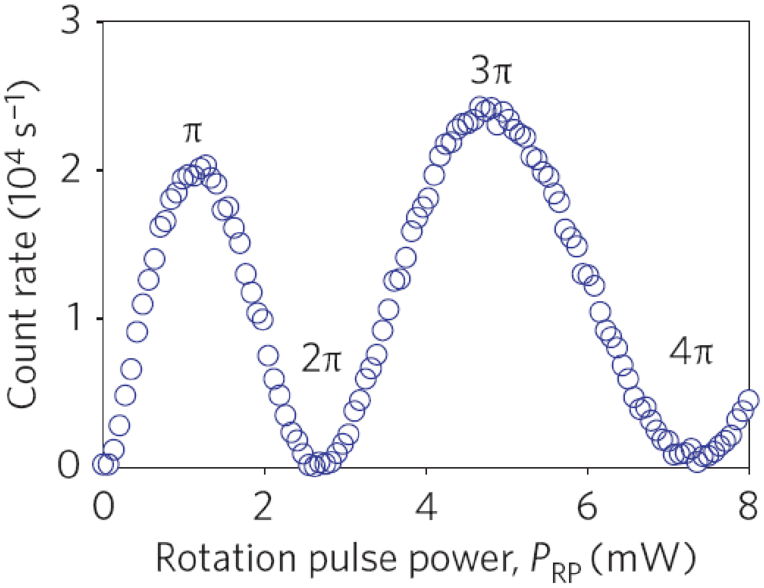

Ramsey Interference experiment

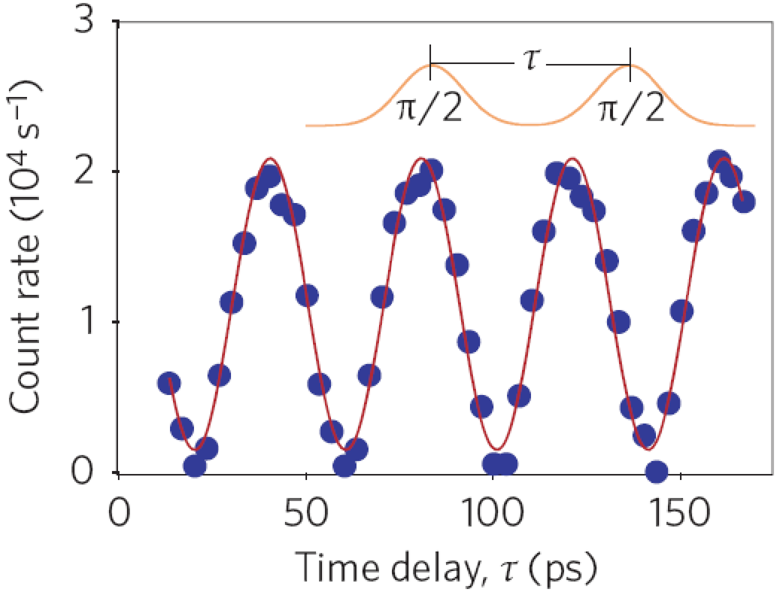

Single qubit gate fidelity: F=98~99%

Outline

- Physical qubits – Quantum dot spin lattice in planar microcavity –
- Motivation – Fault tolerant quantum information processing –
- Qubit initialization and projective measurement
- Single qubit gate
- Two qubit gate
- Decoherence time
- Indistinguishable single photons and entanglement distribution
- Topological surface code architecture

Two Qubit Gate based on Topological Phase

T. Spiller et al, New J. Phys. 8, 30 (2006)

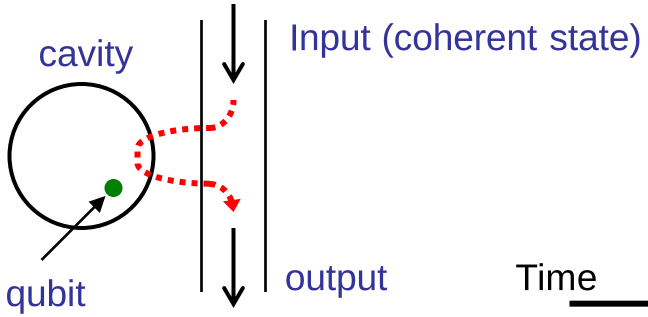

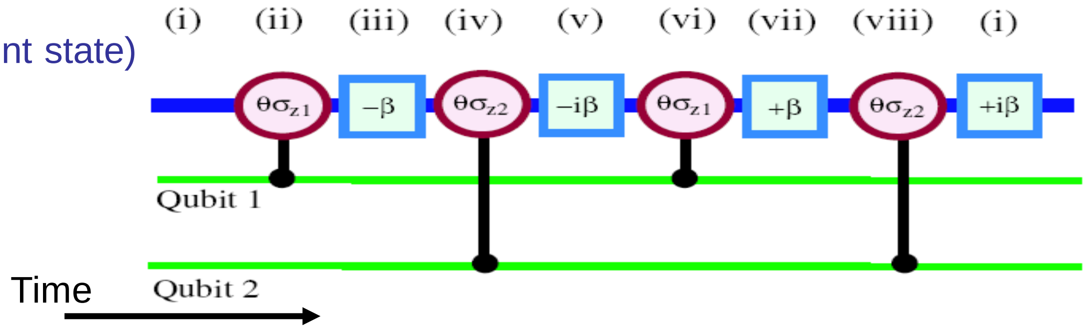

$$\hat{U} = D(i\beta)e^{-in\theta\hat{z}_2/2}D(\beta)e^{-in\theta\hat{z}_1/2}D(-i\beta)e^{-in\theta\hat{z}_2/2}D(-\beta)e^{-in\theta\hat{z}_1/2}$$

$$\beta = \sqrt{2}\alpha e^{-i\pi/4}$$

displacement (beamsplitter)

controlled phase shift (reflection from cavity)

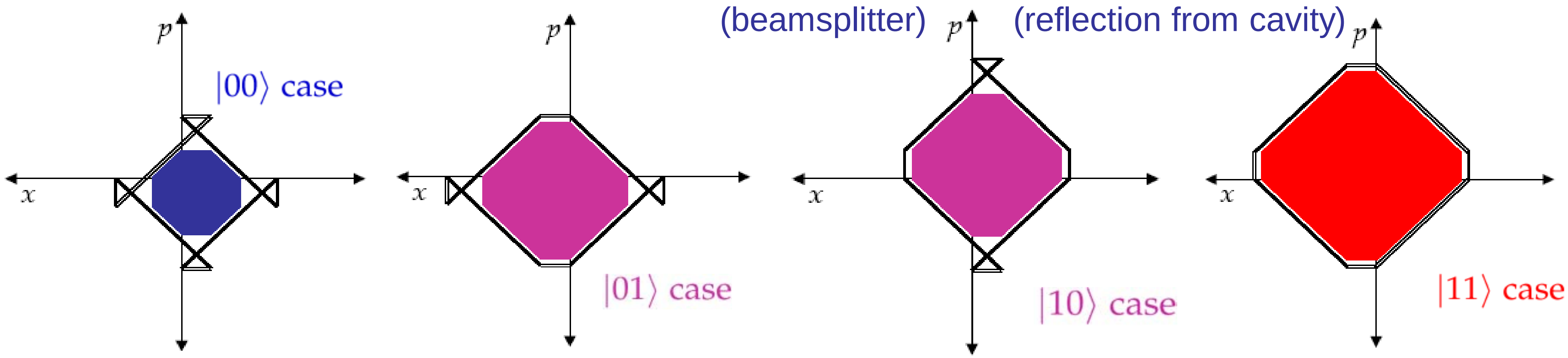

- After the entire sequence, the probe is disentangled from the two qubits.
  ⇨ No measurement and post-selection required.
- An overall phase develops proportional to area (topological phase), $\Phi \simeq 4\alpha^2\theta^2$.
  ⇨ A desired phase shift of π achieved with $\alpha\theta \simeq 1$.

Two Qubit Gate in Dissipative Planar Microcavity

Y. Yamamoto et al., Phys. Scr. T137, 014010 (2009)

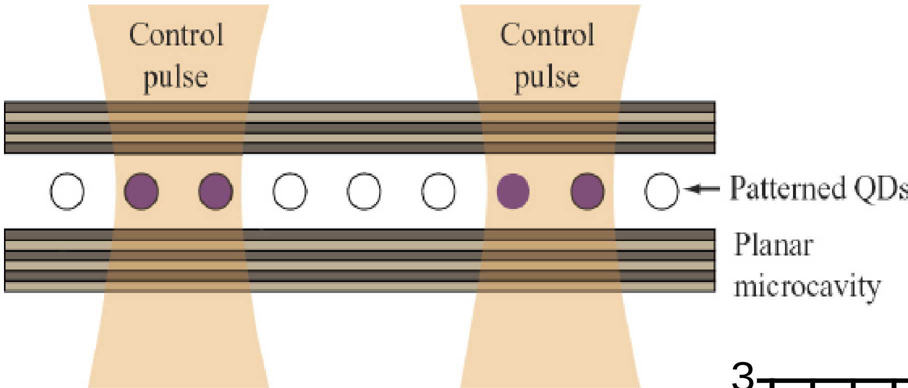

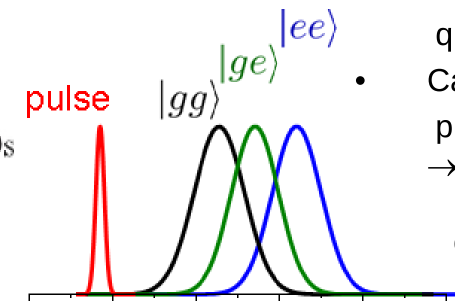

- Cavity resonance depends on qubit states
- Cavity field amplitude by detuned pulse depends on resonance position
  $\rightarrow$ Amplitude "path" of cavity internal field depends on qubit states

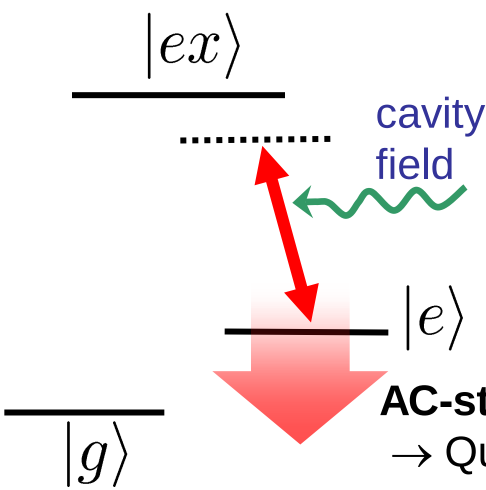

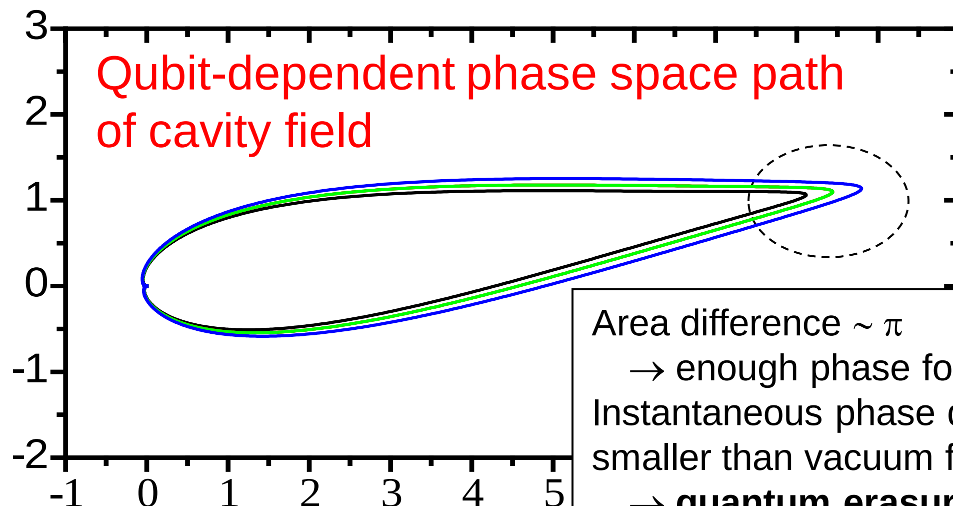

Area difference ~ π
$\rightarrow$ enough phase for CZ gate
Instantaneous phase difference smaller than vacuum fluctuation
$\rightarrow$ **quantum erasure**

AC-stark shift depends on cavity field amplitude

$\rightarrow$ Qubits therefore alter each other's phase

$\rightarrow$ CZ gate for surface code creation

$\rightarrow$ Master equation simulations indicate fidelity>99% with Q=10^5

τ~10nsec (purely optical), τ~100psec (polaritonic)

Outline

- Physical qubits – Quantum dot spin lattice in planar microcavity –

Motivation – Fault tolerant quantum information processing –

- Qubit initialization and projective measurement
- Single qubit gate
- Two qubit gate
- Decoherence time
- Indistinguishable single photons and entanglement distribution
- Topological surface code architecture

T_1 and T_2 Time of Si:GaAs Donor Electron Spins

T1 >4msec at B < 4T

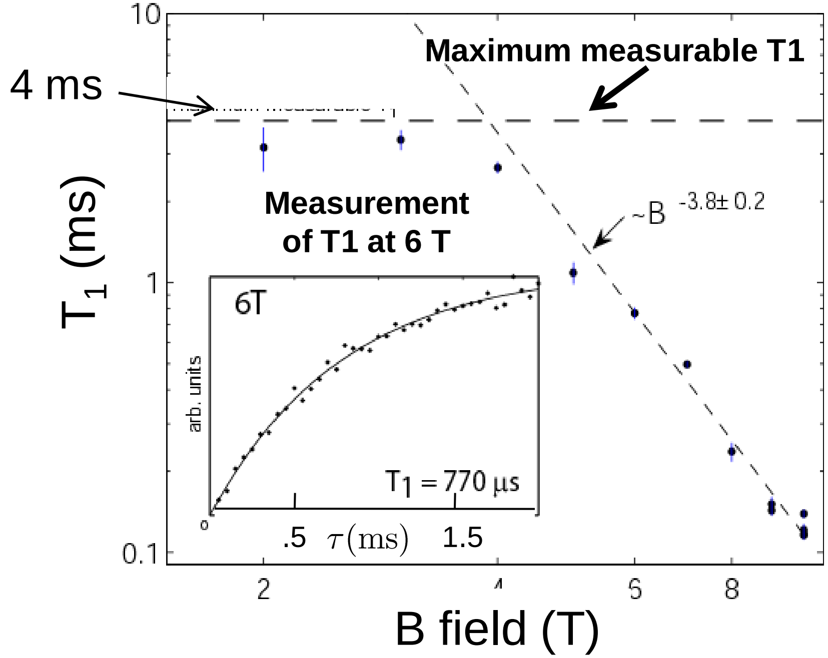

Pulse sequence:

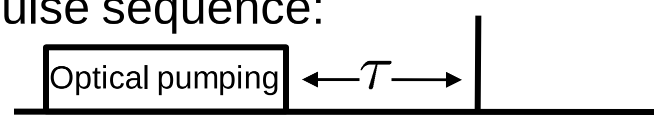

Fu, K.-M. C. et al. PRB 74, 121304 (2006).

T2 ~7μsec at B=10 T and T=1.5K
(small angle spin echo)

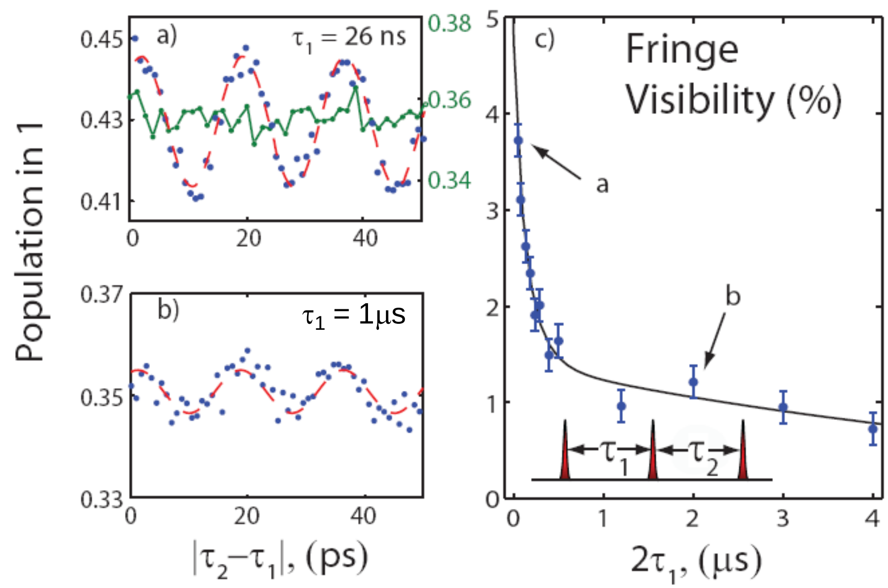

Exponential decay T_2~7μs

(Free induction decay T_2^*~ 1-2ns)

Pulse sequence:

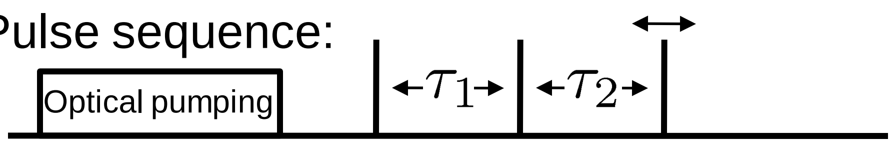

S. Clark. et al. Phys. Rev. Lett. 102, 247601(2009)

Optical Spin Echo Experiment with a Single Spin in a microcavity

D. Press et al., Nature Photonics 4, 367 (2010)

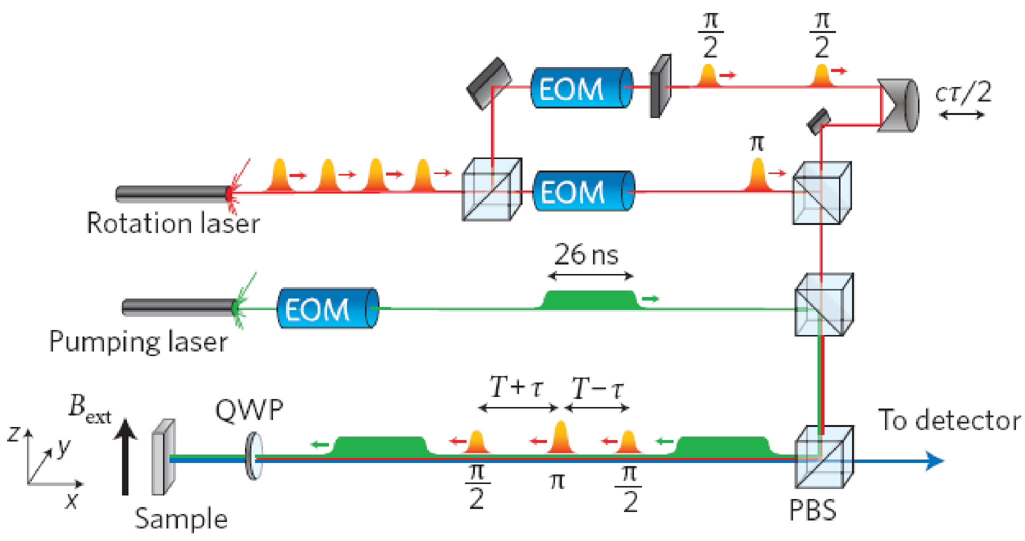

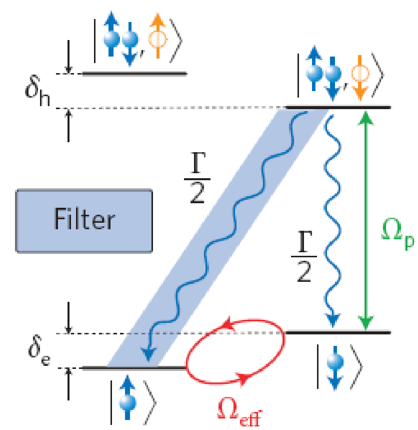

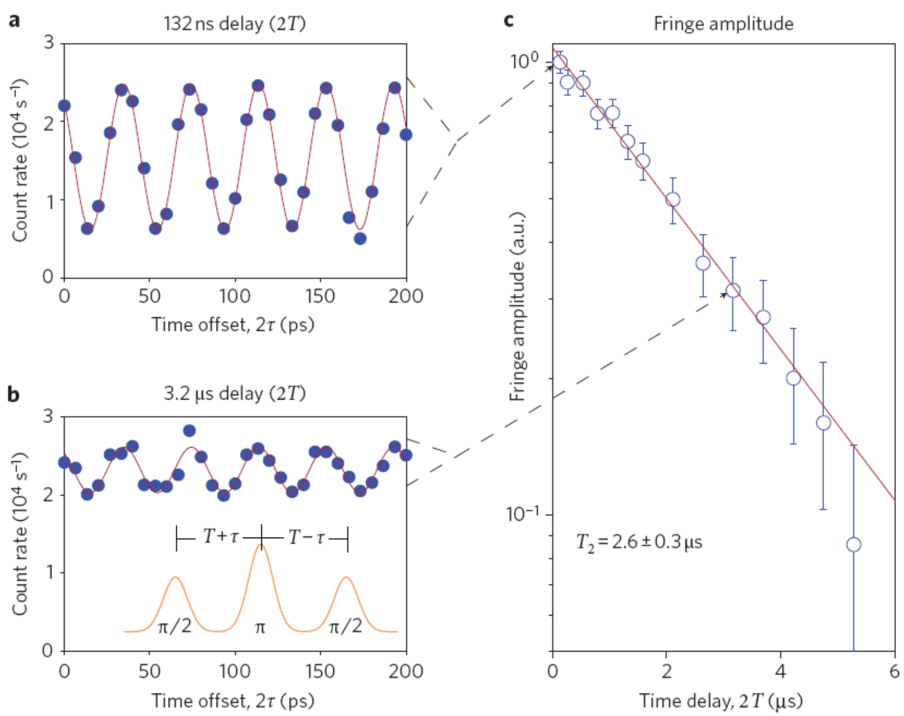

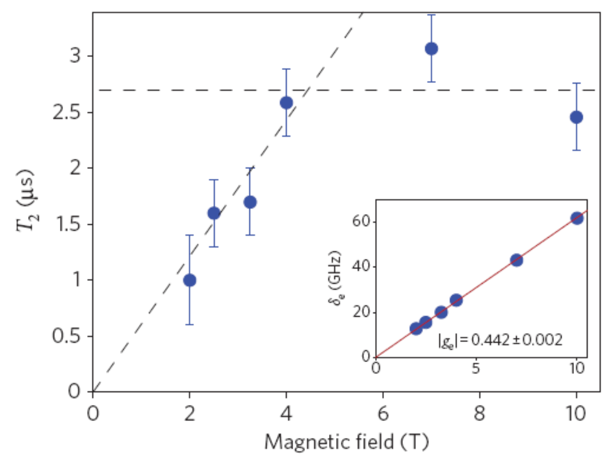

Shorter T_2 observed at B<4T

T_2 =25 sec of ^{29}Si Nuclear Spins in Natural Crystal Silicon
T. Ladd et al., Phys. Rev. B, 71, 014401 (2005)

$$\frac{1}{T_2} = \frac{1}{2T_1} + \frac{\gamma^2}{2}\int_{-\infty}^{\infty} < \Delta H_z(t)\Delta H_z(0) > dt + \left[\left\langle \left[\hat{\mathcal{H}}_D, \left[\hat{\mathcal{H}}_D, \hat{I}_x\right]\right]\right\rangle / \langle \hat{I}_x \rangle\right]^{1/2}$$

natural linewidth

$(\sim 10^{-4}\text{Hz})$

fluctuating local magnetic field along Z-axis at $\omega \simeq 0$

Spin echo (CPMG π -pulse sequence)

dipolar coupling among Iso-nuclear spins

decoupling ($\frac{\pi}{2}$-pulse sequence)

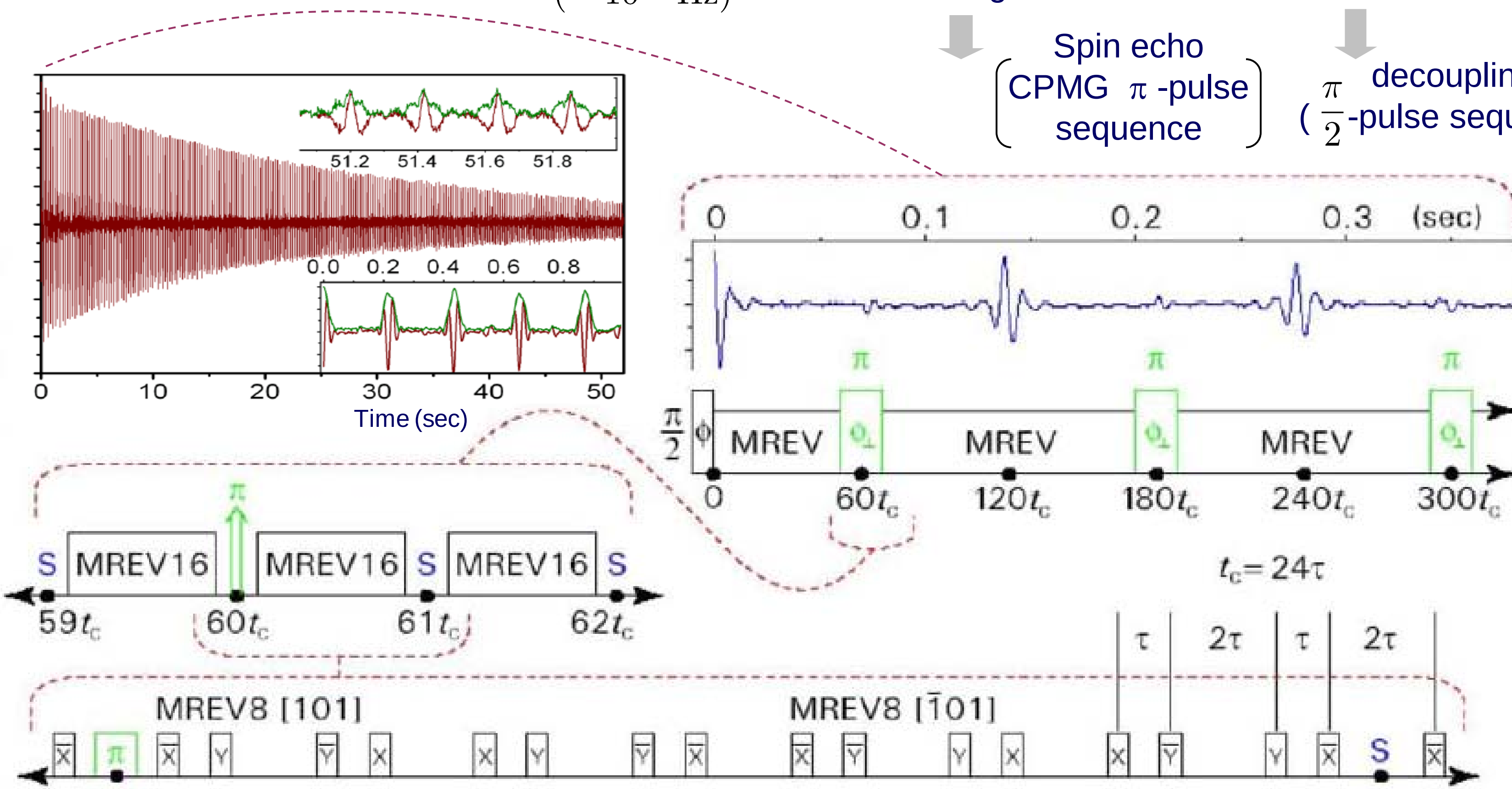

Outline

- Physical qubits – Quantum dot spin lattice in planar microcavity –
- Motivation – Fault tolerant quantum information processing –
- Qubit initialization and projective measurement
- Single qubit gate
- Two qubit gate
- Decoherence time
- Indistinguishable single photons and entanglement distribution
- Topological surface code architecture

Generation of Indistinguishable Single Photons from a Single QD in a Post-Microcavity

C. Santori et al., Nature 419, 594 (2002)

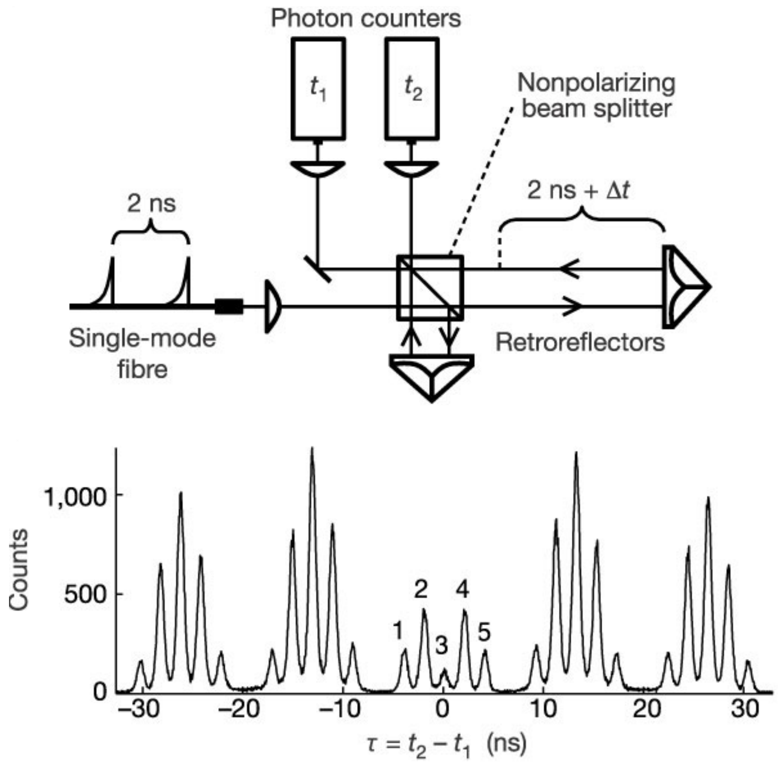

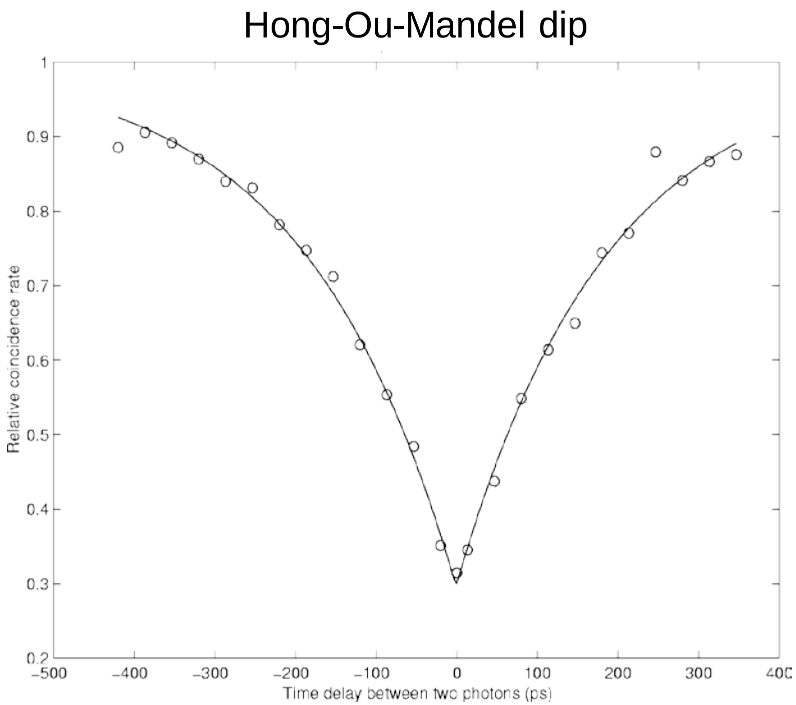

Table 1 **Summary of quantum-dot parameters**

	$g^{(2)}$	g	τ_s (ps)	τ_c (ps)	τ_m (ps)	$V(0)$
Dot 1	0.053	0.039	89	48	80	0.72
Dot 2	0.067	0.027	166	223	187	0.81
Dot 3	0.071	0.025	351	105	378	0.74

Quantum Memory: Clean Atomic Systems in Semiconductors

– Donor Nuclear Spin, Bound Electron Spin (D^0) and Bound Exciton (D^0X) System –

neutral donor bound exciton

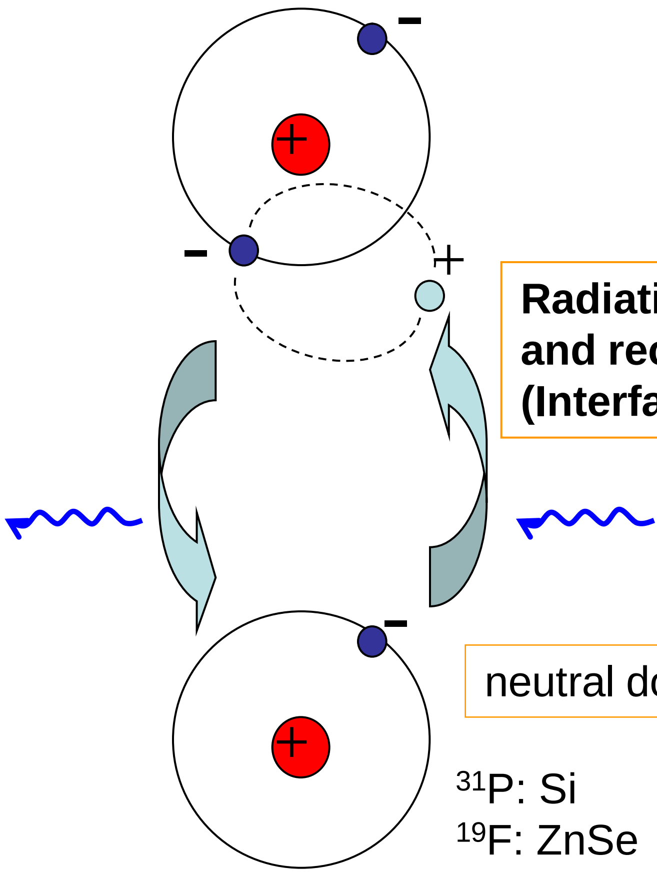

Radiative excitation and recombination (Interface to qubus)

neutral donor

^{31}P: Si
^{19}F: ZnSe
NV center

electron spin with homogeneous g-factor (quantum processor)

simplest nuclear spin –½ (quantum memory)

Background nuclear spins can be depleted for Si and ZnSe by isotope engineering

Diamagnetic shift, Zeeman splitting, Two electron satellite emission

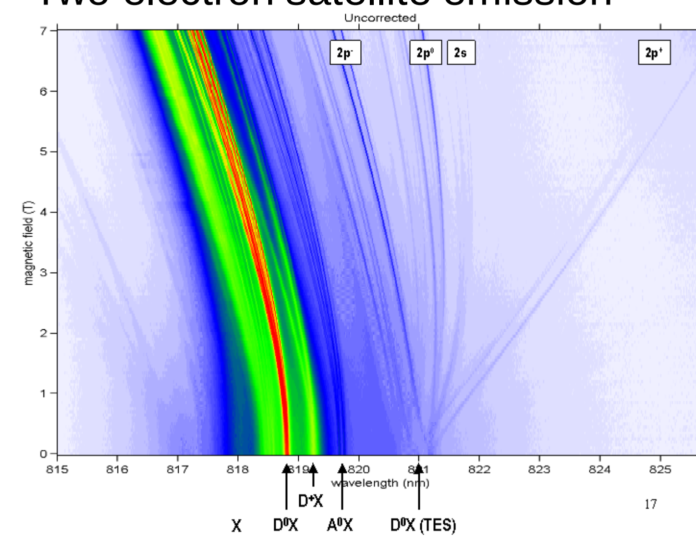

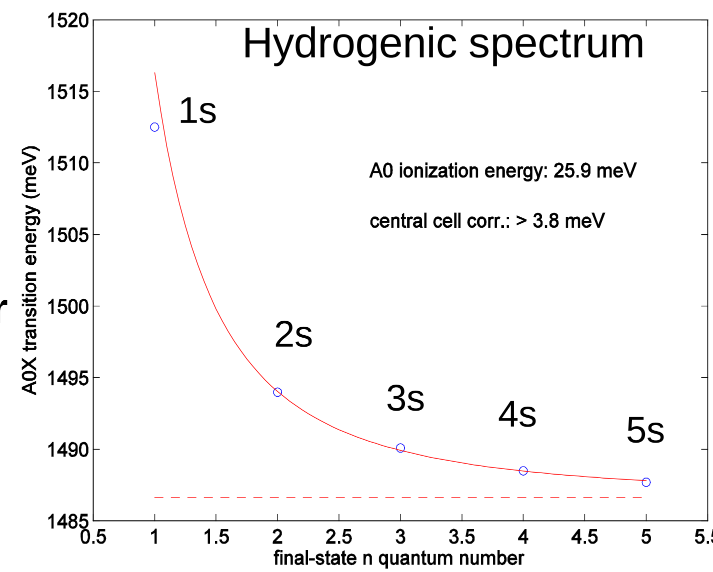

Indistinguishable Single Photons from Two $^{19}F{:}ZnSe$ Donors

K. Sanaka et al., Phys. Rev. Lett. 103, 053601 (2009)

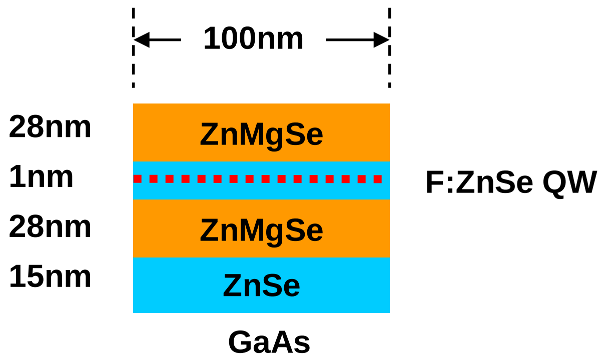

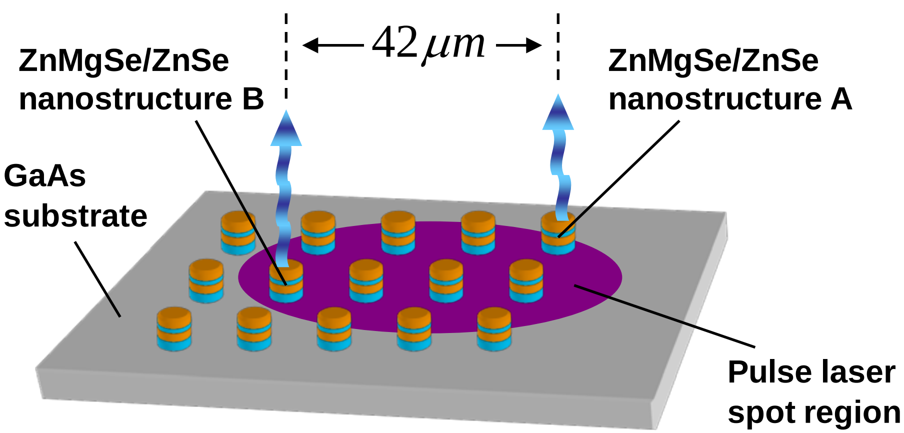

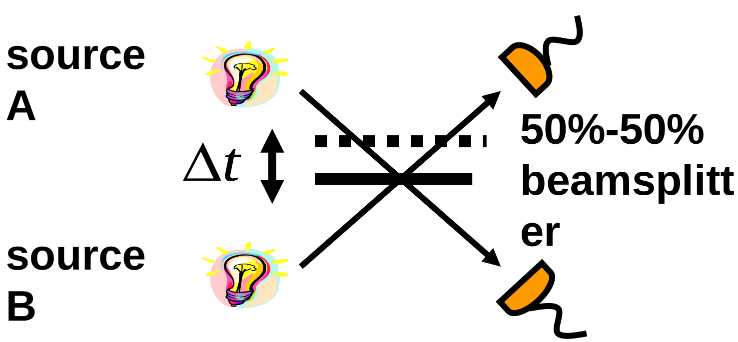

Coincidence count rates as a function of delay time (Hong-Ou-Mandel dip)

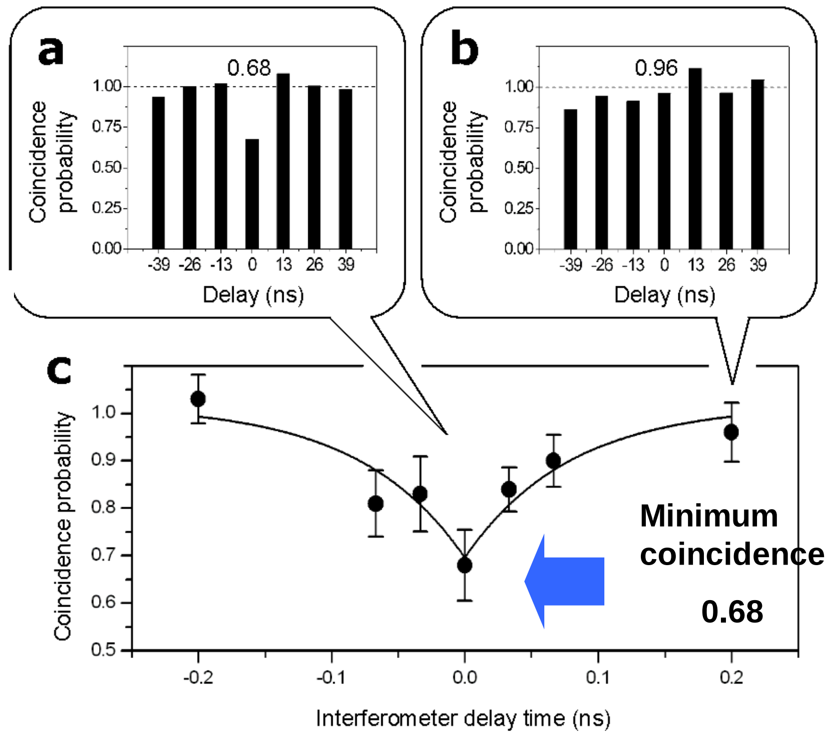

Visibility $$V = \frac{P_C(0.2\text{ns}) - P_C(0)}{P_C(0.2\text{ns})} = 31[\%]$$

Indistinguishability $$I = 65 \pm 13[\%]$$

Coherence time $$\tau_C = 74 \pm 38[\text{ps}]$$

Entanglement Distribution based on Indistinguishable Single Photon Generation and Coincidence Detection

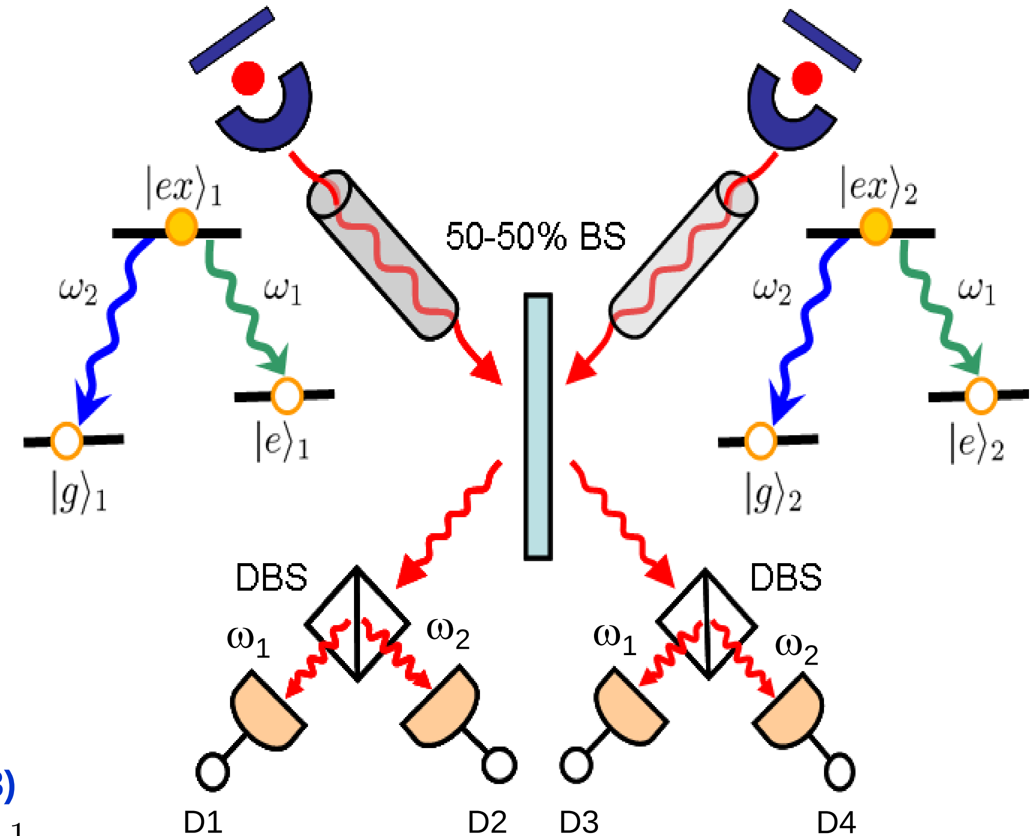

Theory:
C. Simon et al.,
Phys. Rev. Lett. 91, 110405 (2003)

click at D1/D2 or D3/D4 ➡ $\frac{1}{\sqrt{2}}(|e\rangle_1|g\rangle_2 + |g\rangle_1|e\rangle_2)$

click at D1/D4 or D2/D3 ➡ $\frac{1}{\sqrt{2}}(|e\rangle_1|g\rangle_2 - |g\rangle_1|e\rangle_2)$

Experiment with trapped ions:
D.L. Moehring et al., Nature 449, 68 (2007)
S. Olmschenk et al., Science 323, 486 (2009)

Outline

- Physical qubits – Quantum dot spin lattice in planar microcavity –
- Motivation – Fault tolerant quantum information processing –
- Qubit initialization and projective measurement
- Single qubit gate
- Two qubit gate
- Decoherence time
- Indistinguishable single photons and entanglement distribution
- Topological surface code architecture

Layered Architecture for Fault-Tolerant Quantum Computation

– How to Construct a Perfect Quantum Computer out of Imperfect Quantum Devices –

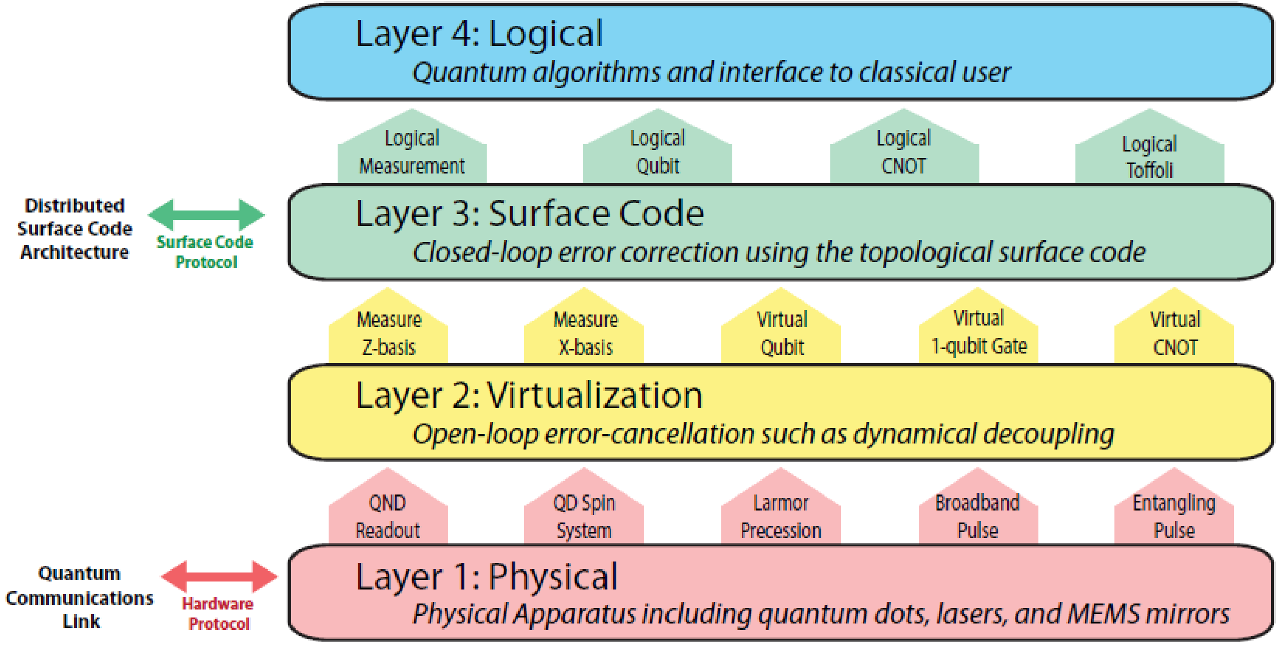

QuDOS
(Quantum Dots with
Optically controlled Spins)

- Each layer has a prescribed set of duties to accomplish.
- A lower layer provides the services to the one above it.
- An above layer issues commands to the layer below and processes the results.

Isolation of design problems in individual layers and independent evolution of layers.

Layer 1 : Physical

**Mission: Storage and manipulation of unprotected quantum information
Provides the essential physical resources to satisfy the virtualization layer**

Tools:

- Storage – Electron spin state in 2D square array of charged quantum dots in a planar microcavity
- Qubit – Zeeman sub-levels in a transverse magnetic field (Voigt geometry)
- Initialization/Measurement – Single shot QND readout of the spin state (➡ Detector array with integrated CMOS processors)
- Single qubit gate – Ultra-fast optical pulse rotates the spin vector
- Two qubit gate – Cavity photon or polariton mediates the nearest neighbor spin-spin coupling (➡ Entangling operation)

Enemies:

- Decoherence
- Dynamic coherent (systematic) and incoherent (random) errors (gate errors)

Layer 2 : Virtualization

Mission: Storage and manipulation of protected quantum information

- Open-loop systematic error cancellation – Refocusing and dynamical decoupling
- Virtual qubit above layer 2 appears to be a static qubit
- Virtual gate – Composite pulse sequences realize virtual qubit states with reduced error from layer 1 processes to satisfy the threshold of the surface code (gate error < 0.7%)

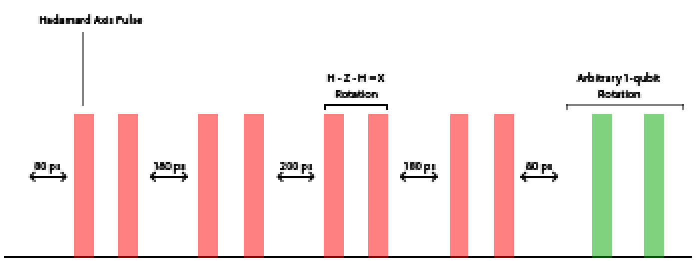

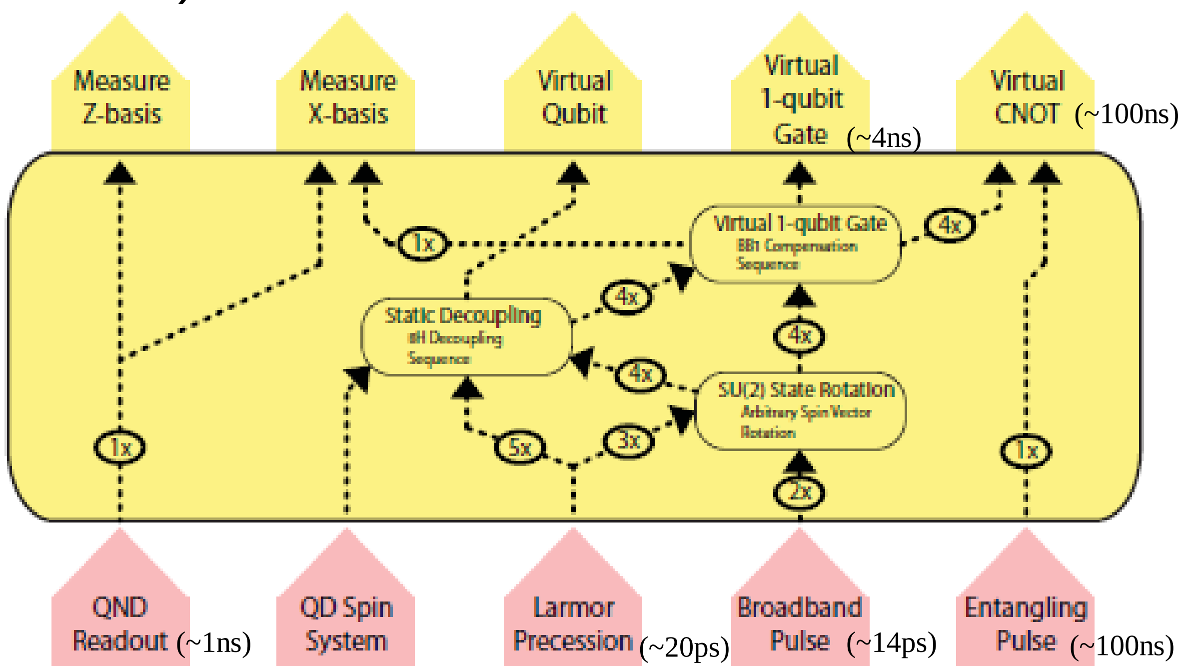

Layer 3 : Surface Code

Mission: Correct arbitrary errors with quantum error correction [R. Raussendorf, J. Harrignton and K. Goyal, NJP 9 (2007)]

- Logical qubit = Defect in the surface code
- Closed loop error correction – Periodically measure an error syndrome and use Pauli frame (X, Y, Z or I) instead of error correction
  ⇒ interpretation of final result
- Error threshold for fault-tolerance – 0.75% for virtual qubits and gates
  Error ⇒ determine code size

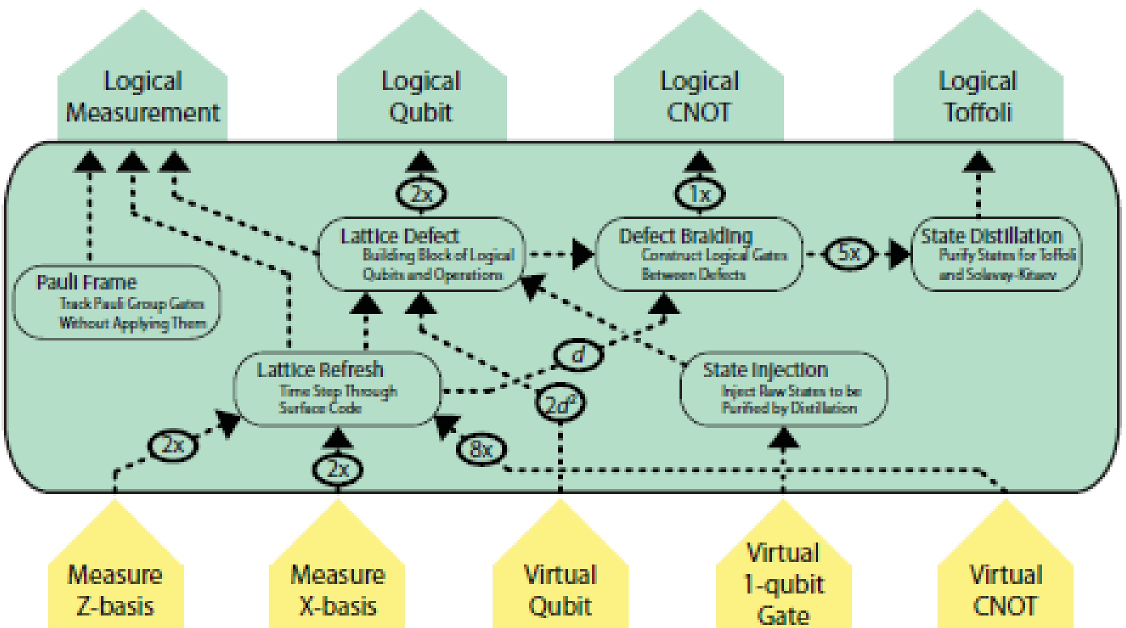

- Injection of single qubit states
- 2D array of qubits with NN coupling (CNOT)
- Measurement in X and Z bases

Size and Operation Time of Surface Code

Shor's factoring algorithm for 2048-bit integer

Parameter	Symbol	Value
Threshold error per virtual gate	ϵ_{thresh}	7.5×10^{-3}
Error per virtual gate	ϵ_V	1×10^{-3}
Number of logical gates	K	9×10^{12}
Number of logical qubits	Q	12288
Error per logical gate	ϵ_L	9×10^{-20}
Surface code distance	d	53
Virtual qubits per logical qubit		19600

Operation	**Label**	**Composition**	**Max Duration**
Lattice Refresh with Alternating Phase Masks	LatticeRefresh	$2 \times (\mathtt{IZ} \cdot 4 \times \mathtt{CNOT} \cdot \mathtt{MZ} \cdot \mathtt{IX} \cdot 4 \times \mathtt{CNOT} \cdot \mathtt{MX})$	1.61 μs
Defect Braiding	DefectBraid	30 × LatticeRefresh	48.4 μs
Logical CNOT	LogicalCNOT	3 × DefectBraid	145 μs
State Distillation	StateDistill	5 × DefectBraid	242 μs
Logical Toffoli Gate	LogicalToffoli	14 × DefectBraid	678 μs

# of logical qubits Q ~ 6N

Success probability of quantum algorithm

~99.99%

↓

$\varepsilon_L \leq 10^{-4}/KQ$

↓

code distance 53

total number of physical qubits

2 x 10^8 (minimum)

~ 10^9 (sufficient)

Virtual Gates in a Surface Code Refresh Step

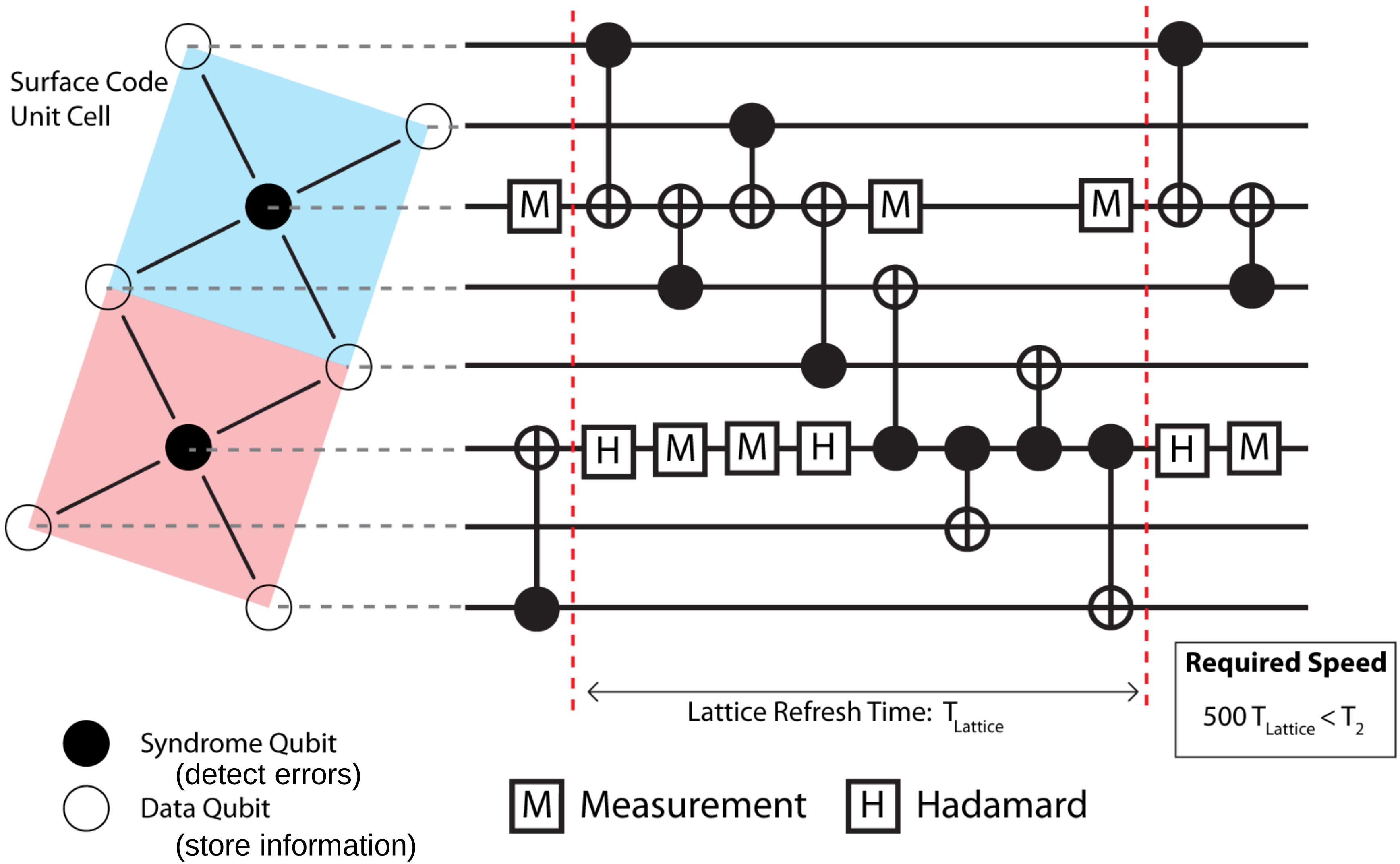

A lattice refresh cycle of the surface code can be performed in parallel across the entire 2D array of virtual qubits.

Layer 4 : Logical

Mission: Execute the quantum algorithm on the logical qubits provided by the surface code and output the end result in a classical form

- 2048-bit number factoring – 14 days in contrast to ≳ 1000 years in classical computers

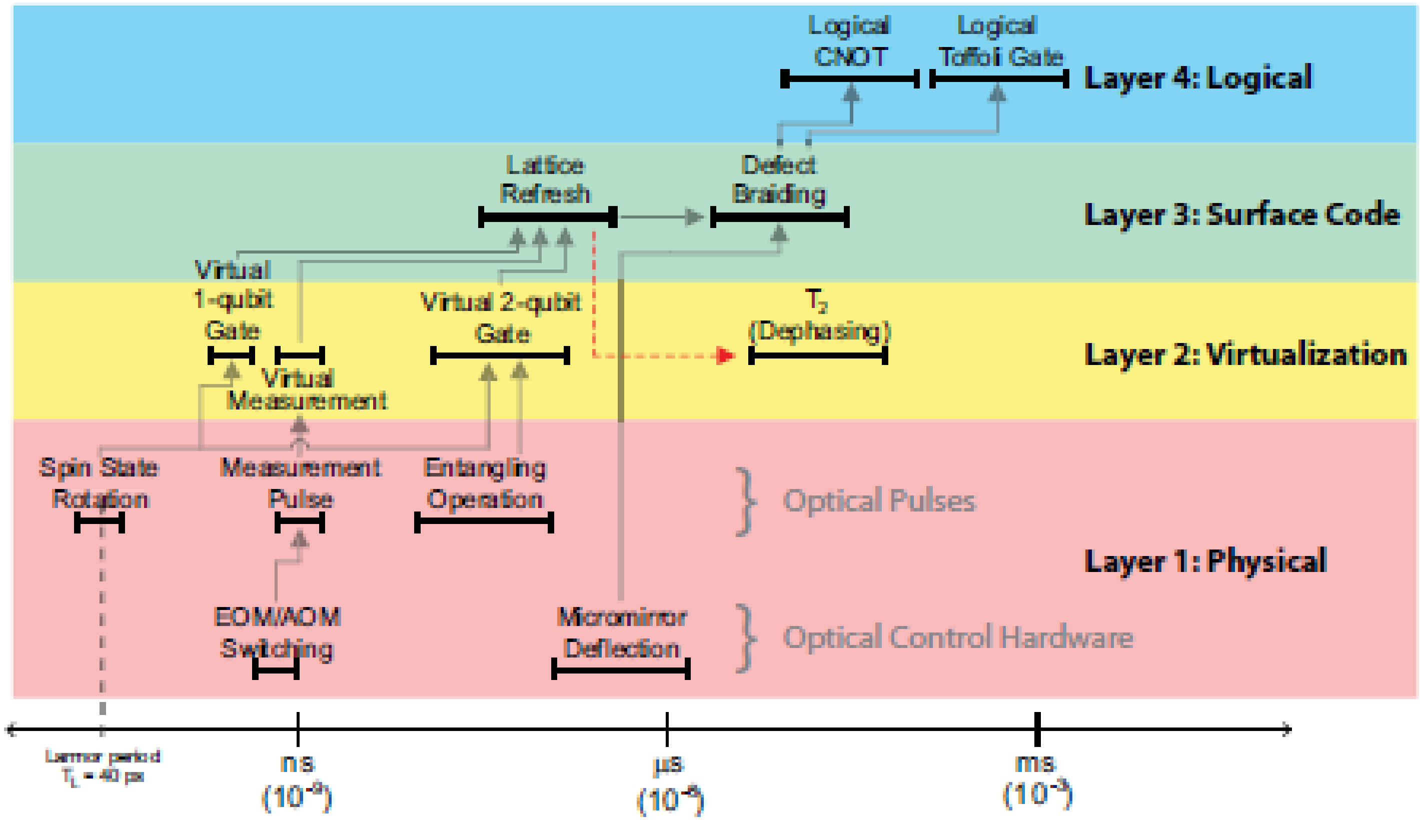

Primary Control Loop of the Surface Code Quantum Computer

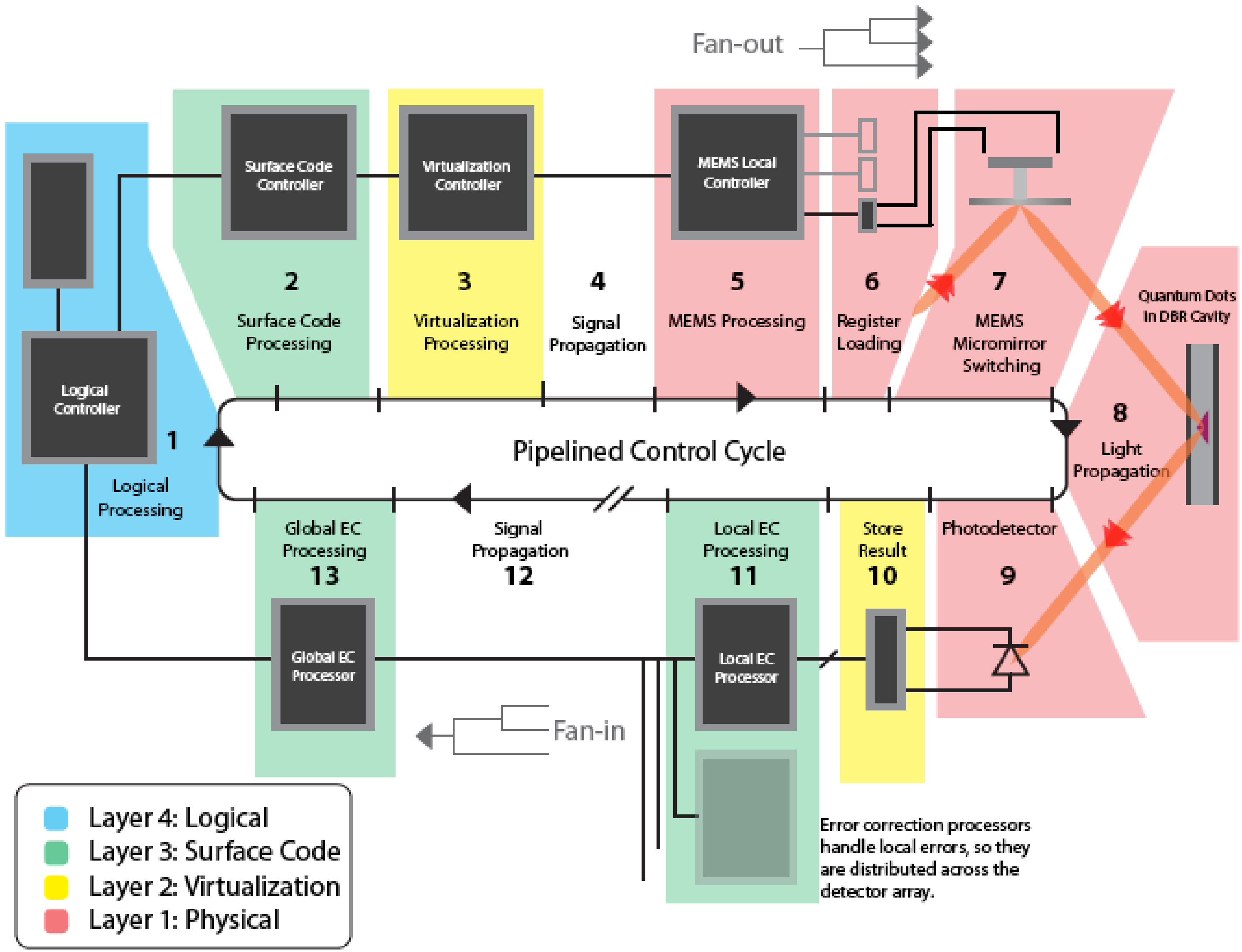

Resource requirement for Shor's factoring machine
— n= 2,048-bit number —

40ps one-bit/1ns two-bit gates, 99.9% fidelity, 3us coherence time
60n~120,000 logical qubits
code distance d=30 ⇨ ~10^8 physical qubits
computational time: 100-1000 years by classical methods
⇨ ~5 hours by this quantum computer

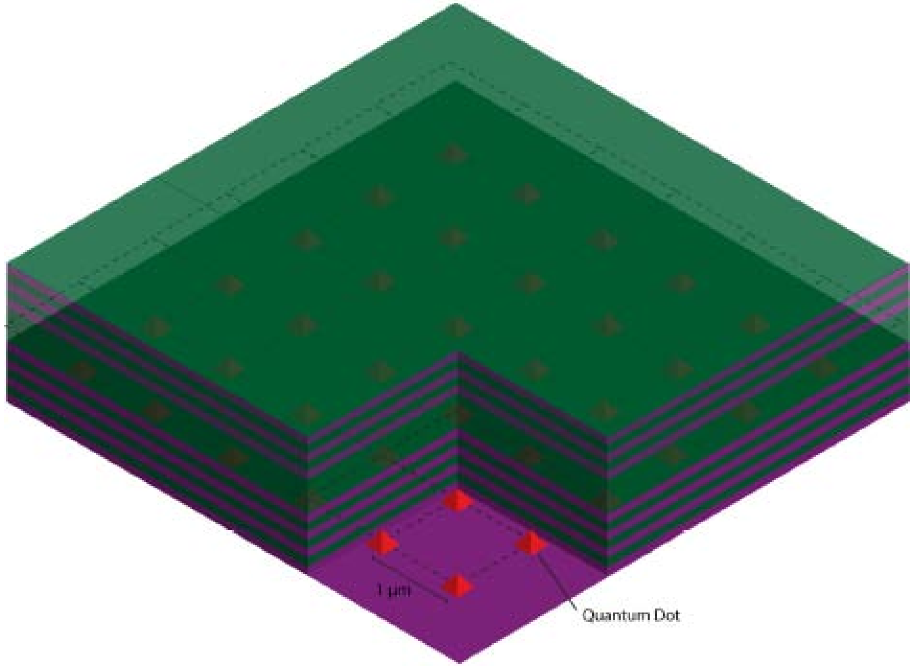

This number of QDs can be implemented in 2D square lattice with ~1μm QD spacing on $1cm^2$ chip.

Summary and Outlook

Essential elements for semiconductor spin-based quantum information processing

- ☑ Initialization in ~3nsec with F=92%
- ☑ Single qubit gate in ≲ 20 psec with F=98-99%
- ☑ Decoherence time $T_2 \sim 3\mu$sec

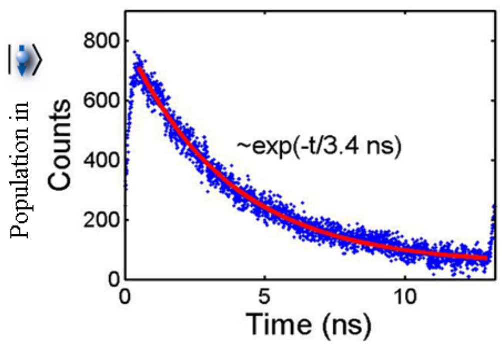

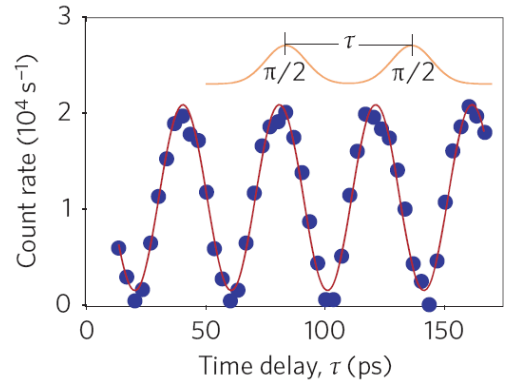

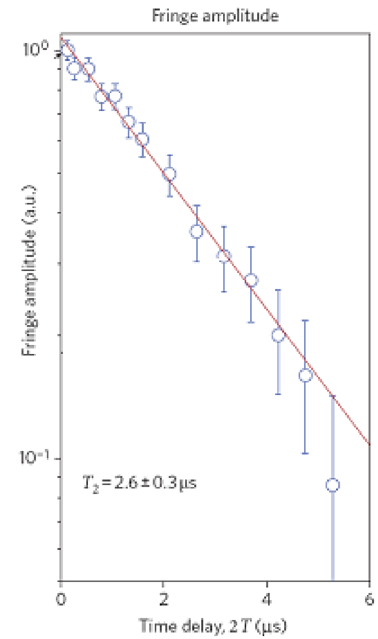

- ☐ Two qubit gate by single optical pulses

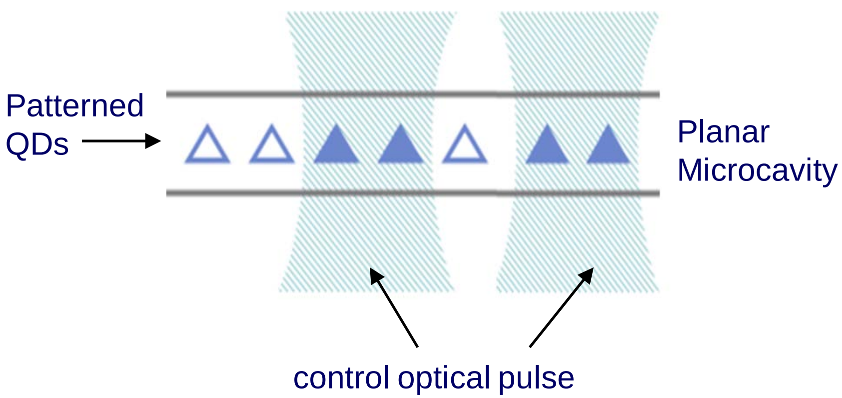

- ☐ Entanglement distribution by coincidence detection of indistinguishable single photons

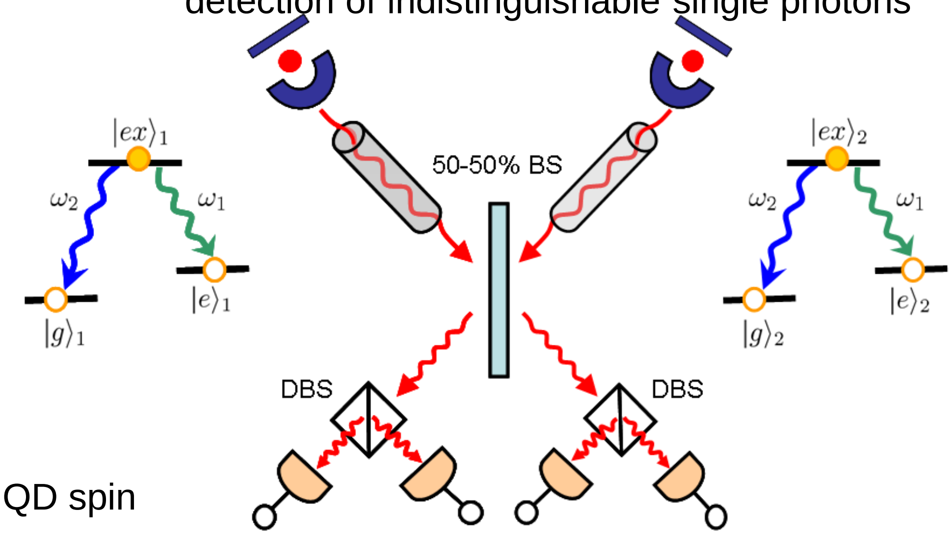

- ☐ Single shot QND measurement of a single QD spin